## VII. Conclusion

In conclusion, the single oscillator transceiver gave good performance. In spite of its simple circuit configuration, it had superior characteristics with regard to loss and distortion of the frequency up-conversion function as compared with conventional equipment having TX-local oscillator, an up-converter and a RX-local oscillator.

The waveguide circuits, which determine the equipment's cost, are greatly reduced, to about half those of the conventional equipment. Furthermore, the newly developed IMPATT diode mount with disk-hat type resonator provides stable operation and good adjustability.

The single oscillator transceiver is one solution to the problem of finding effective low-cost light-density local trunking radio equipment for intracity applications.

## Acknowledgment

We would like to express our sincere thanks to Dr. S. Aoi and Y. Masuda, who gave the opportunity for research and development, and K. Kaminishi, who developed the semiconductor devices for this 40-GHz band radio equipment, and also to T. Iwano, H. Nakano, S. Endo, S. Gotoh, and Y. Fujita, who supported the development.

## References

[1] P. T. Greiling and G. I. Haddad, "Large signal equivalent circuits of avalanche transit time devices," *IEEE Trans. Microwave Theory Tech.*, vol. MTT-18, pp. 842–853, Nov. 1970.

[2] R. K. Gupta and C. G. Englefield, "Up-Conversion in IMPATT amplifiers," *IEEE Trans. Microwave Theory Tech.*, vol. MTT-26 pp. 28–30, Jan. 1978.

[3] M. Hata, A. Fukasawa, M. Bessho, S. Makino, and M. Higuchi, "A new 40 GHz digital distribution radio with single local oscillator," *MTT-Int. Microwave Symp.*, B4.1, June 1978.

[4] G. Cachier and J. Espaignol, "The pretuned module: An integrated millimeter wave oscillator," ISSCC 77, 11.7, 1977.

[5] K. Nawata, "Studies on equivalent circuits of resonant-hat type IMPATT oscillators,"*Trans. IECE* (Japan), vol. J60-C no. 10, Oct. 1977.

[6] K. Tajima, O. Kurita, and H. Suzuki, "Hat-type Impatt-diode amplifiers and their stabilization," Microwave Meet. IECE Japan, MW78-45, 1978.

[7] K. Shirahata and K. Ogiso, "Stabilization of solid-state microwave oscillators by loading BPF," *Trans. IECE* (Japan), vol. 54-B, no. 11, Nov. 1971.

[8] T. Ohta and M. Hata, "Noise reduction of oscillators by injection locking," *Trans. IECE* (Japan), vol. 53-B, no. 9, Sept. 1970.

[9] W. J. Evans and G. I. Haddad, "Frequency conversion in IMPATT Diodes," *IEEE Trans. Electron Devices*, vol. ED-16, pp. 78–87, Jan. 1969.

[10] H. Shiota, K. Kohiyama, and S. Kita, "A frequency stabilized self-oscillating converter using solid-state oscillators," *Trans. IECE* (Japan), vol. J55-B, no. 12, pp. 691–692, Dec. 1972.

# Practical Considerations in the Design of a High-Power 1-mm Gyromonotron

JOSEPH DOV SILVERSTEIN, MEMBER, IEEE, MICHAEL E. READ, KWO RAY CHU, AND ADAM T. DROBOT

*Abstract*—A second harmonic gyromonotron has been designed to have an output of 4 kW at a frequency of 240 GHz, and to operate with an overall efficiency of 14 percent. The design method utilized a detailed theory of the gyrotron oscillator and an electron orbit computer code. Particular attention was paid to the problem of mode competition in the oscillator cavity. Although a particular design example is considered, the method is of general interest.

## I. Introduction

D uring the past several years the gyrotron [1] has been shown to be an efficient source (4–45 percent) of high-power radiation (1 kW–1 MW) at wavelengths less than 1 cm. Although a number of such devices have been

operated successfully in the U.S. in the 8–10-mm range, [2], [3], the only devices operating in the near-millimeter wave range ($\lesssim 3$ mm) are those built in the Soviet Union [4], [5].

This paper describes results of the design phase of the first known effort in the U.S. to build an efficient high-power gyrotron oscillator operating with a wavelength near 1 mm. Specifically, the design goals for this gyromonotron (i.e., single-cavity cyclotron resonance maser (CRM)) were 1–10 kW (peak) at 1.3. mm and an overall efficiency of 10–15 percent. It was to operate at the second harmonic of the cyclotron frequency ($\omega \simeq 2\Omega_c$) and with a cavity mode of $TE_{051}$. Although these last two facts allow operation at reduced magnetic field and higher power than would be possible with the fundamental and lower order modes, they greatly increase the problem of mode competition; the circumvention of this complication is one of the main considerations in this design.
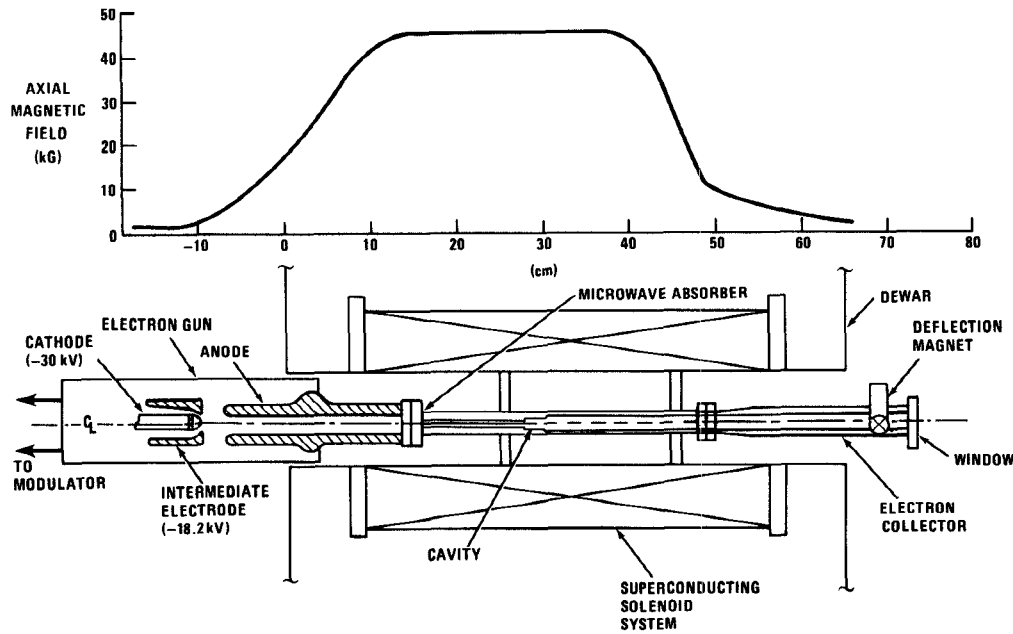
Fig. 1. Schematic of 240-GHz gyrotron oscillator and plot of axial magnetic field.

## II. DESIGN CONSIDERATIONS

A schematic of the device is shown in Fig. 1. The design utilized both analytical and numerical methods. For the beam-wave coupling and oscillation start conditions, the linear theory of Chu [6] was used. Calculation and optimization of the device efficiency required the use of a code initially developed by Drobot [7], and modified by the authors.

The desired output of the device was 1–10 kW at the frequency of 240 GHz. An operating mode of the class of $TE_{0nl}$ was considered desirable because of the ease with which other modes can be preferentially damped [8]. In addition, these modes are well suited to a high-power device, since wall losses in the cavity and output waveguides are minimal for modes without azimuthal variations. The value of $n$ was chosen to be 5 to allow a large enough cavity radius to minimize breakdown or heating problems and reduce perturbations caused by machining errors, while allowing operation near cutoff. (The latter is necessary for optimum CRM coupling [1].) It is desirable to operate at as low a cyclotron harmonic as possible in order to minimize mode competition. Since the maximum magnetic field available was 60 kG, the minimum possible cyclotron harmonic $S$, and the one chosen, was 2.

The initial ratio of perpendicular to parallel electron momentum $\alpha$, important because only the perpendicular energy is available to the cyclotron resonance maser interaction, has an upper limit fixed by present electron-gun technology. A reasonable estimate for this limit, without knowledge of the exact gun design, appeared to be 1.5 [9]. Finally, the beam voltage was chosen to be $V = 30$ kV, a value deemed to be practical for nonlaboratory devices.

The linear theory allowed calculation of the beam-wave coupling, which is inversely proportional to the product of electron beam power $P$ and cavity $Q$ required for an oscillation to start. The parameters varied in these calcula-
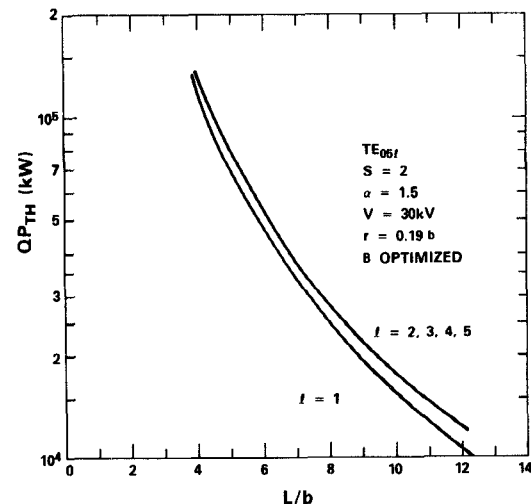


Fig. 2. Threshold $QP$ for gyrotron oscillator versus cavity length-to-radius ratios from gyrotron cavity theory. $(QP)_{th}$ for $l=2,3,4,5$ have nearly the same value so they are represented by the same curve.

tions were $L$ (cavity length), $r$ (mean beam radius), and $l$ (axial eigennumber of the cavity mode). There are several locally optimum values of $r$. The strongest coupling occurs for the smallest of these values [6], $r=0.19b$, where $b$ is the cavity wall radius. This value therefore requires the lowest starting current and, despite the small beam radius, yielded the smallest spread in velocities due to space charge. As seen in Fig. 2, the mode $l=1$ has stronger coupling than modes for which $l>1$, and the choice for that parameter was so determined.

## III. EFFICIENCY OPTIMIZATION

The optimization of the device efficiency was then carried out by varying the remaining parameters $L, I$ (beam current), $Q_L$ (leakage $Q$), and $B$ (external magnetic

field), with the boundary conditions as follows:

$$Q_L > 4\pi(L/\lambda)^2 \tag{1}$$

$$I_{th} < I < 2A \tag{2}$$

$$\delta\Delta = \delta\left[\left(\omega - kv_\parallel - \frac{S\Omega_c}{\gamma}\right)\tau\right] \ll 2.5\pi \tag{3}$$

$$Q_L < Q_{\text{ohmic}} . \tag{4}$$

The authors' output power requirement meant that

$$10^3 W < VI < 10^4 W. \tag{5}$$

The condition in (1) states that the leakage $Q$ has a lower limit, usually termed the diffraction $Q$. The condition in (2) states that $I$ must exceed the minimum current required for start of oscillation and be less than 2 A. The latter upper limit on $I$ is imposed by the predicted dependence of electron velocity spread on current density at the cathode of the electron gun [11]. In the present case this upper limit is less than the maximum allowed by voltage depression due to space charge in the cavity. Equation (3) is the criterion given by Chu [6] on the maximum allowed spread in the phase shift $\Delta$ between cyclotron and electromagnetic (cavity) modes. In this equation $\tau = L/v_\parallel$, $v_\parallel$ is the velocity parallel to the magnetic field, $k = \pi l/L$, $\omega$ and $\Omega_c$ are the radiation and relativistic cyclotron frequencies, respectively, and $\gamma$ is the normalized electron energy. Finally, the condition in (4) must be satisfied in order for the ohmic losses to be small.

The code used for the optimization integrates the electron energy loss along its orbit. It is a single particle, three-dimensional code, and calculations are made with steady-state cold cavity field profiles. Optimization was accomplished in a three parameter space, the parameters being $L$, $B$, and $QI$. The parameters $L$ and $B$ determine the phase shift $\Delta$ in (3), and the parameter $QI$, when combined with $\eta_{\text{CRM}}$ (CRM efficiency) and the cavity mode and geometry, yields a measure of the magnitude of electromagnetic fields in the cavity.

The results of the optimization runs for CRM efficiency $\eta_{\text{CRM}}$, versus $QI$, with $\Delta$ as parameter and $L = 8b$, are shown in Fig. 3. We note that the variation of $\eta_{\text{CRM}}$ with field amplitude predicted by the code for small amplitudes is in excellent agreement with that given by the linear theory. The threshold values $(QI)_{th}$ from the linear theory are indicated by the vertical lines in Fig. 3.

The results for maximum CRM efficiency $\eta_{\text{CRM}}^{\text{max}}$, obtained by varying $B$ and $QI$ for various fixed values of $L$, are shown in Fig. 4. It can be seen that $\eta_{\text{CRM}}^{\text{max}}$ has a value of 30 percent for a cavity length $L = 4b$. However, the overall (loaded) efficiency $\eta_L$, unlike $\eta_{\text{CRM}}$, depends on wall losses. It is therefore limited by the boundary conditions (1)–(5) and the maximum achievable ohmic $Q$ of 20 000 in a copper cavity at room temperature. The result is that the highest value of $\eta_L$ is achieved with a cavity length $L = 8b$, even though $\eta_{\text{CRM}}^{\text{max}}$ for this cavity length is only 22 percent. This cavity length was therefore chosen
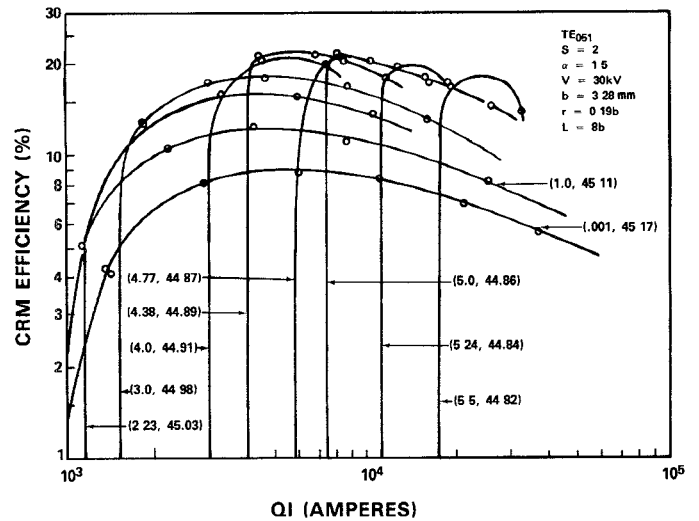


Fig. 3. CRM efficiency versus $QI$ from electron orbit computer code. The two numbers in the parentheses are, respectively, $\Delta$, in radians and $B$, in kilogauss.
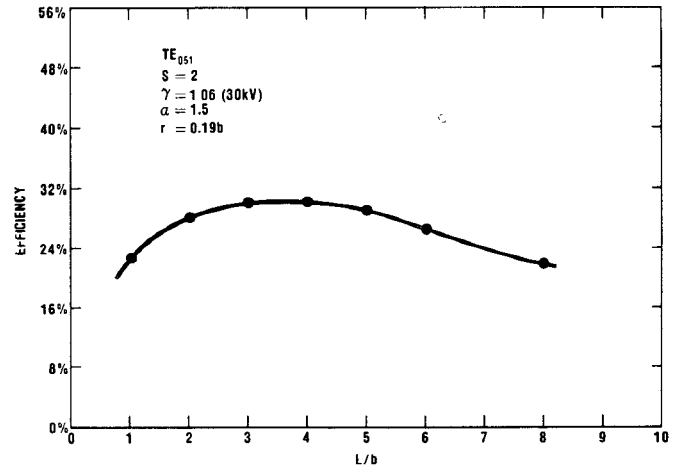


Fig. 4. Maximum CRM efficiency versus cavity length-to-radius ratio from electron orbit computer code.

for the design. From Fig. 3, a $QI$ value of $8.0 \times 10^3$ A maximizes $\eta_{\text{CRM}}$. Assuming an achievable $Q_L$ of 7300 (1.3 times the diffraction $Q$), the total $Q$ of the cavity is 5300, resulting in a required beam current of 1.5 A; $\eta_L$ is then 16 percent.

Our predictions of efficiency versus $QI$ for this gyromonotron have been compared with those based on data from the theory of Nusinovich and Erm [10]. This theory assumes that the RF electric field in the cavity has a Gaussian dependence on axial distance. Such a field shape is known to result in a higher efficiency than the purely sinusoidal shape of a straight cylindrical cavity. The lowest $QI$ for which a comparison could be made by extrapolating the Nusinovich and Erm data is 1.55 $\times 10^4$ A. Assuming an ohmic $Q$ of 20 000 as above, a total $Q$ of 7000, and therefore, a current of 2.2 A, those data predict an $\eta_L$ of 16 percent whereas our simulation code predicts an $\eta_L$ of 11 percent.

The geometry, beam parameters, and magnetic field determine the phase shift $\Delta$ given by (3). Fig. 3 shows that the mechanism is "strong" for $0 < \Delta < 4.5$. This agrees with the analytical theory [6] that strong coupling occurs within the range $-\pi/2 < \Delta < 2\pi$. It is clear that for the stable operation of a device, the phase shift associated with any electrons should not be outside this range. Preferably, the range should be much less than $2.5\pi$. This puts a limit on the inhomogeneity in the static magnetic field and on the electron gun-dependent beam temperature.

The computer code results of Fig. 3 show that in order for this device to operate within 10 percent of its maximum efficiency, spread in the magnetic field should be no greater than 0.2 percent. Other runs with the computer code were made in which the electron velocity components were varied, with the electron energy, applied magnetic field, and RF field amplitude held constant. Based on these runs, the 22-percent CRM efficiency for zero spread in $v_\parallel$ would be reduced to 21 percent for a 10-percent spread in $v_\parallel$ and to 20 percent for a 20-percent spread in $v_\parallel$.

## IV. MODE COMPETITION

Until now it has been assumed that the cavity can only oscillate in the $TE_{051}$ mode. In order to assess the effects of mode competition, $(QI)_{th}$ for other $TE_{0nl}$ modes was calculated by means of the linear theory at values of $\Delta$ for those modes corresponding to the range in $\Delta$ for the $TE_{051}$, $S = 2$ mode in Fig. 3. Values of $S$ ranging from 1 through 3 were scanned. As was expected, $(QI)_{th}$ for a number of $TE_{0nl}$, $S = 1$ modes was less than that for the $TE_{051}$, $S = 2$ mode due to the stronger coupling at the first cyclotron harmonic than at the second. However, due to the rather strong dependence of $\Delta$ on resonant frequency (see (3)), the only modes with $S = 1$ for which the requirement $-\pi/2 < \Delta < 2\pi$ was satisfied were those with rather large axial mode number $l$. Assuming a coupling scheme in which $Q_L$ has the previously stated value of 7300 for $TE_{051}$, the value of $Q_L$ for modes with larger $l$ is correspondingly smaller [8]. The result is that for the entire range in $\Delta$ or $B$ over which the gyrotron would be operated for oscillation in the $TE_{051}$, $S = 2$ mode, the lowest $S = 1$ mode threshold power, which occurs for the $TE_{028}$ mode, is still about ten times that of the $TE_{051}$, $S = 2$ mode. The only modes whose threshold power is comparable to that of the $TE_{051}$, $S = 2$ mode are other $TE_{05l}$, $S = 2$ modes.

The results for $P_{th}$ versus $\Delta$ or $B$ are shown in Fig. 5. It is seen that while the $TE_{051}$ mode has the lowest threshold for high magnetic fields, the $TE_{052}$ mode has a lower threshold for $B = 44.86$ kG, the field for which the $TE_{051}$ mode is most efficient, as is evident from Fig. 3. In order to assure stable operation in this mode, a reasonable operating point is probably 44.98 kG. Fig. 3 then shows that $\eta_{CRM}$ is reduced from 22 percent to 18 percent, leading to a reduction in $\eta_L$ from 16 percent to 13 percent.
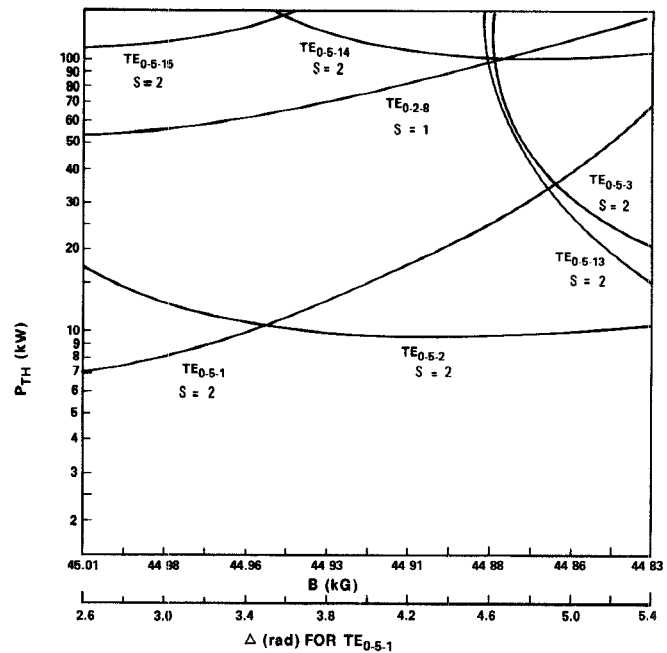


Fig. 5. Threshold power for gyrotron oscillation in various modes versus $B$ from gyrotron cavity theory. $Q_L = 7300$ for the $TE_{051}$ mode.

### TABLE I
### GYROMONOTRON PARAMETERS

| | |
|---|---|
| Frequency | 240 GHz |
| Cavity mode | $TE_{051}$ |
| Output power | 3.5 kW |
| Cavity diameter $\times$ length | $6.6 \times 26.2$ mm |
| Beam voltage | 30 kV |
| Beam current | 0.9 A |
| Beam geometry | annular |
| Mean beam diameter | 1.2 mm |
| Initial ratio of electron perpendicular to parallel momentum in cavity | 1.5 |
| Beam thickness | 0.2 mm |
| Magnetic field | 45 kG |
| Magnetic field homogeneity in cavity | 0.2 percent |
| Beam temperature: | |
| Axial component | 10 percent |
| Transverse component | 5 percent |

The device parameters resulting from the design are given in Table I.

## REFERENCES

[1] V. A. Flyagin, A. V. Gaponov, M. I. Petelin, and V. K. Yulpatov, "The gyrotron," *IEEE Trans. Microwave Theory Tech.*, vol. MTT-25, pp. 514–521, June 1977.

[2] M. Read, L. Seftor, R. Lucey, K. R. Chu, and J. D. Silverstein, "A high power 35 GHz microwave source for ECRH," in *Conf. Record (Abstracts) 1978 IEEE Int. Conf. Plasma Science*, p. 302.

[3] H. Jory, S. Hegji, J. Shivley, and R. Symons, "Gyrotron developments," *Microwave J.*, vol. 21, no. 8, pp. 30–32, Aug. 1978.

[4] N. I. Zaytsev, T. B. Pankratova, M. I. Petelin, and V. A. Flyagin, "Millimeter and submillimeter-wave gyrotrons," *Radio Eng. Electron. Phys.* (USSR), vol. 19, no. 5, pp. 103–107, May 1974.

[5] A. A. Andronov, V. A. Flyagin, A. V. Gaponov, A. L. Gol'den-berg, M. I. Petelin, V. G. Usov, and V. K. Ulpatov, "The gyrotron: High power source of millimeter and submillimeter waves," *Infrared Phys.*, vol. 18, no. 5/6, pp. 385–393, Dec. 1978.

[6] K. R. Chu, "Theory of electron cyclotron maser interactions in a cavity at the harmonic frequencies," *Phys. Fluids*, vol. 21, pp. 2354–2364, Dec. 1978.

[7] P. Sprangle and A. T. Drobot, "The linear and self-consistent nonlinear theory of the electron cyclotron maser instability," *IEEE Trans. Microwave Theory Tech.*, vol. MTT-25, pp. 528–544, June 1977.

[8] M. Read, R. M. Gilgenbach, R. Lucey, K. R. Chu, J. Silverstein,

and V. L. Granatstein, "Spatial and temporal coherence of a 35 GHz gyromonotron operating in the $TE_{01}$ mode," Naval Res. Lab., Washington, DC, NRL Memorandum Rep. 4244, June, 1980.

[9] L. Seftor, A. Drobot, and K. R. Chu, "An investigation of a magnetron injection electron gun suitable for use in a cyclotron resonance maser," Naval Res. Lab., Washington, DC, NRL Memorandum Rep. 3697, July, 1978.

[10] A. V. Gaponov, A. L. Gol'denberg, D. P. Grigor'ev, T. B. Pankratova, M. I. Petelin, and V. A. Flyagin, "Experimental investigation of centimeter-band gyrotrons," *Radiophys. Quant. Electron.*, vol. 18, no. 2, pp. 204–211, Feb. 1975.

[11] Varian Assoc., private communication.

# Hybrid Integrated Frequency Doublers and Triplers to 300 and 450 GHz

TOHRU TAKADA, TAKASHI MAKIMURA, AND MASAMICHI OHMORI, MEMBER, IEEE

*Abstract*—High-power wide-band submillimeter-wave frequency sources have been developed. A frequency doubler to 300 GHz has delivered an output power of 5 mW with 3-dB-down bandwidth of more than 10 GHz. A frequency tripler to 450 GHz with an output power of 0.5 mW has also been tested. These multiplier output powers are highest values in the respective frequency regions up to date.

The successful performances have been achieved by use of GaAs Schottky-barrier diodes and hybrid integrated circuits which are specially designed to obtain high output power.

## I. INTRODUCTION

In recent years, the submillimeter-wave region has been investigated in the fields of radio astronomy, plasma diagnostics, spectroscopy, and Josephson detector research [1].

The authors and others have succeeded in obtaining frequency sources operating at up to 600 GHz by using frequency multipliers with GaAs Schottky-barrier diodes [2]. At 300 GHz, the obtained power was 0.7 mW by the hybrid integrated doubler [3] and 2 mW by the double ridged type tripler [4]. At 450 GHz, the output power was 0.12 mW by the hybrid integrated tripler [2]. However, these output power levels were too small compared with the power levels that were handled in the lower frequency regions for use in many applications and the output bandwidths were too narrow.

In order to increase the output power of the submillimeter-wave multipliers, a special design, which is different from that in the millimeter wave region, is necessary. In the millimeter wave region, the multiplier performance primarily depends upon a diode figure of merit (diode cutoff frequency $f_{cb}$). The performance in the submillimeter wave region, however, is decided by an external circuit as well as $f_{cb}$ due to the increased circuit loss and the difficulty of circuit impedance matching.

The authors designed and fabricated the multipliers, while paying attention to the above points, and obtained 5- and 0.5-mW output power readings in 300- and 450-GHz regions, respectively. In addition, the doubler to 300 GHz has shown wide-band characteristic with 3 dB-down width of more than 10 GHz.

This paper describes the diode and circuit designs, the fabrication techniques, the performances of the doubler to 300 GHz, and the measurement results for the tripler to 450 GHz.

## II. DIODE DESIGN AND FABRICATION

A flow chart of the high-power multiplier fabrication sequence is shown in Fig. 1. The design and fabrication of the diode are described in the following, according to the flow chart.

### A. Diode Fabrication

A principle of the frequency multiplier is harmonic generation by use of variable capacitance of the diode